JOURNAL OF CATALYSIS **119**, 135–145 (1989)

Methane Conversion and Fischer–Tropsch Catalysis over MoS_2: Predictions and Interpretations from Molecular Orbital Theory

ALFRED B. ANDERSON AND JENWEI YU

Chemistry Department, Case Western Reserve University, Cleveland, Ohio 44106

Received September 28, 1988; revised April 10, 1989

An atom superposition and electron delocalization molecular orbital study has been made of a variety of CH_n and CO reactions over coordinatively unsaturated Mo^{IV} edge cations in MoS_2. CH_3, formed by oxidative insertion of an edge Mo into a CH_4 bond, is found to dehydrogenate easily by means of H transfer to an adjacent Mo. The process is activated by the formation of a strong double bond between CH_2 and Mo. Couplings of 2 CH_3, CH_3 + CH_2, and 2 CH_2 are found to proceed with high barriers, a consequence of electron promotion to the Fermi level during C–C bond formation, yielding unstable C_2 species. Coupling to strongly adsorbed ethylene proceeds with the lowest barrier, and if ethylene forms hydrogenation to ethane is possible, although ethane formation from 2 CH_4 is thermodynamically forbidden so none of these CH_n coupling schemes will be productive in the absence of stabilizing ancillary reactions. CO is found to bind relatively weakly to fivefold coordinated Mo and strongly to fourfold coordinated sites. In the presence of a second adjacent fourfold coordinated Mo, CO easily tilts to the di-σ bridging orientation and dissociates with a low barrier. In the Fischer–Tropsch process hydrogenation to $CH_3(a)$ and $H_2O(g)$ is expected. CO is found to insert into the Mo–CH_3 bond, as found by Klier and co-workers, with a low barrier, and subsequent hydrogenations to form C_2H_6 + H_2O or CH_3CH_2OH are found to be favorable. It is proposed that the selectivity toward alcohol formation over alkali-doped MoS_2 (the DOW process) may stem from the ability of the alkali cations to bond to O from the CO insertion process, thus blocking hydrogenation to H_2O, which would lead to alkane products.

INTRODUCTION

An important goal for chemists is finding new ways to selectively oxidize methane. Methane C–H bond activation has in recent years been found to proceed more easily on transition metal centers than believed originally (*1*), and there is hope for the discovery of useful homogeneous catalytic methane oxidation processes.

Heterogeneous processes have been known for a number of years and center mostly around activation by oxides to form methanol and lesser amounts of other low-molecular-weight products (*2*). The role of O^- as a hydrogen abstractor at the catalyst surfaces has been analyzed theoretically (*3*). Clean metal surfaces can activate C–H bonds (*4a, 4b*) but as yet the formation of graphite fibers by iron particles (*4a*) is perhaps the only controlled process that has developed using metals. The oxidative addition of methane to metal surfaces has been examined theoretically (*5*).

Molybdenum disulfide is an interesting catalyst with the ability to isomerize hydrocarbon molecules (*6*), hydrogenate olfeins (*7*), and form C_1–C_5 alkanes and alcohols from hydrogen and carbon monoxide in a Fischer–Tropsch process (*8*). In a recent theoretical study it was found that fourfold coordinated Mo^{IV} at the edge of MoS_2 crystal layers, which are short by 2 from the bulk Mo^{IV} coordination number of 6, possess the ability to activate methane to yield coordinated CH_3 and H. This process was essentially oxidative addition, with the Mo inserting into a methane C–H bond. As discussed in another theoretical study (*9*), this H should be able to transfer to neighboring edge S^{2-}, resulting in heterolytic H^+ and CH_3^- adsorption products. Since the pro-

0021-9517/89 $3.00

cess is close to energy neutral, for it to occur in practice should require a high CH_4 pressure. Whereas H_2 adsorption can lead to H· migration over the S^{2-} surface layers and formation of a bronze (*10*), in the case of methane the binding of $CH_3\cdot$ to S^{2-} was too weak for this to happen, so methane's heterolytic adsorption products will stay at the edge and migration of H^+ over the S^{2-} surface will be retarded by its electrostatic attraction to the neighborhood of its CH_3^- partner. It is of interest to explore the coupling of two such CH_3^- species to form ethane. This is similar to the coupling of CH_3 chemisorbed on metal surfaces as studied by Zheng *et al.* (*11*) and one expects a high activation energy because of the energy it takes to promote the two anion electrons (the vehicle is the C–C σ^* orbital that forms and becomes less stable as the C–C σ bond forms) to the Fermi level to reduce the metal, in this case Mo^{IV}.

In our earlier study of methane activation on MoS_2 (*12*) it was found that dehydrogenation of adsorbed CH_3 to yield coordinated methylene, CH_2, and H was energetically possible. Barriers to migration from one four-coordinate Mo^{IV} site to another were found to be low, with CH_2 the more mobile species. This suggested that CH_2 + CH_2 coupling to ethylene and CH_2 + CH_3 coupling to ethyl might occur, and it is of interest to examine these processes, the latter of which is expected to follow a pathway of CH_2 insertion into the Mo–CH_3 bond.

In thinking about the formation of heavier hydrocarbon molecules from CH_4 by the above processes, it must be noted that the reactions to form H_2 + C_2H_4, C_2H_6, and so on are uphill in enthalpy and free energy. If the H_2 could be oxidized to H_2O by passing O_2 + CH_4 over MoS_2, the formation of C_2H_n would be thermodynamically allowed, but oxidation of the MoS_2 becomes a potential problem. Adding H_2 and H_2S to the reactants might serve to keep the MoS_2 reduced and render the process catalytic. However, this process will not be studied here. Rather, the C_1 coupling reactions mentioned above will be examined using molecular orbital theory.

The Fischer–Tropsch activity of MoS_2 and alkali-doped MoS_2, the former leading to alkane and the latter to alcohol production, is of particular interest, for it suggests the possibility of consuming CH_4 in these processes, assuming that it is activated as described above. A mechanism for CH_4 consumption can then be suggested following recent work of Klier and co-workers (*13*), who used ^{13}C-labeled CO and found that C_n chain growth in Fischer–Tropsch synthesis over MoS_2 and alkali-doped MoS_2 follows an insertion mechanism where CO inserts into the Mo–alkyl bond. In their work the alkyl species is formed by hydrogenation of CO, but what if it can be formed by dissociative adsorption of CH_4? The reaction

$$CH_4 + CO + 2H_2 \rightarrow C_2H_6 + H_2O$$

has a standard enthalpy change of −1.46 eV and the standard free energy change is also negative. Consequently, a theoretical study of CO insertion into the Mo–CH_3 bond and the formation of C_2H_6 and C_2H_5OH is made in this paper. The effect of alkali on favoring the alcohol product route in Fischer–Tropsch synthesis over MoS_2 is also addressed, and it is suggested that K^+ may bind to O in the inserted CO, preventing its hydration and loss as H_2O.

THEORETICAL METHOD

The atom superposition and electron delocalization molecular orbital (ASED-MO) theory (*14, 15*) and cluster models are employed. The ASED-MO method is based on a physical model of partitioning molecular electronic charge density functions into free atom components and the remainder, which is an electron delocalization density. By integrating the electrostatic forces on the nuclei as atoms bind, one obtains, within this density function partitioning, two-body atom–atom repulsive energies due to atom superposition and attractive energies due to electron delocalization. In the ASED-MO method the repulsive components are evaluated for the nucleus of the more electropositive atom of each pair and the attractive components are approximated by an orbital energy stabilization which is calculated by use of a Hamiltonian similar to extend Hückel. Diagonal matrix elements are set equal to the negative of the experimental valence state ionization potentials (VSIP), and off-diagonal matrix elements are the average of the diagonal elements multiplied by $2.25S_{ij}\ \exp(-0.13R)$ where S_{ij} is the overlap integral of the two orbitals on different centers and R is the internuclear distance. Off-diagonal matrix elements for atomic orbitals on the same nuclear center are set equal to zero. Slater orbitals are used, double ζ for transition metal atoms and single ζ for others. The VSIP are shifted to yield reasonable charge transfers and the exponents are changed to yield bond lengths. Usually such adjustments are made for diatomic fragments and the resulting parameters are then used for studying the larger systems. In this way charge self-consistency and relativistic core effects on valence orbital sizes are taken into account. Parameters were thus chosen in an earlier study (*12*), and are given in Table 1.

The MoS$_2$ edge site cluster models used in this work have excess S, so electrons are added to the cluster molecular orbitals to ensure band occupation as in the bulk. These electrons do not affect the Hamiltonian matrix elements or the calculated electronic structure.

The molecular and transition state structures given below were optimized using 0.01 Å and 1° steps in distance and angle variables. By optimizing the structure of the reacting system for each of a series of internuclear distances for the bonds being formed, it is believed that the lowest energy transition state structures have been found within the tetrahedral angle assumption given below. ASED-MO calculations overestimate C–H and C–C bond lengths as follows: C–H, 0.1 Å; C–C, 0.2 Å; C═C, 0.15 Å; and C≡C, 0.1 Å; O–H and C–O bond lengths are within 0.1 Å of the actual values. Dissociation energies calculated in this work are D_e values, which omit corrections for zero-point vibrations. Figures give calculated distances and angles, except for the calculated C–H bond lengths of 1.21 Å for all CH$_3$ groups, 1.19 Å for CH$_2$(a), and 1.20 Å for C$_2$H$_4$(a). Tetrahedral angles are assumed for adsorbed methyl and ethyl species and for the ethanol molecule and its adsorbed precursers. For ethane and ethanol the respective calculated C–C bond lengths are 1.75 and 1.74 Å. In ethanol the C–O length is 1.43 Å, the αH–C lengths are 1.23 Å, and the O–H length is 0.99 Å.

This work is best viewed as a guide to probable reaction mechanisms. The orbital

TABLE 1

Parameters Used in the Calculations: Principal Quantum Number, n; Orbital Ionization Potential, IP; Slater Orbital Exponents, ζ; and Corresponding Linear Coefficients, c

Atom	*s*			*p*			*d*					
	n	IP (eV)	ζ (a.u.)	n	IP (eV)	ζ (a.u.)	n	IP (eV)	ζ_1 (a.u.)	ζ_2 (a.u.)	$c1$	$c2$
H	1	11.1	1.2									
C	2	14.09	1.658	2	8.76	1.618						
O	2	25.98	2.246	2	11.12	2.227						
S	3	19.50	2.022	3	9.66	1.727						
Mo	5	7.80	1.956	5	4.62	1.656	4	9.26	4.542	1.701	0.60814	0.60814

correlation diagrams help give an understanding of the electronic factors associated with activation processes and bond strengths. The adsorption energies and energy changes for various steps discussed in this work have uncertainties. For example, CH_4 coupling over MoS_2 is estimated to be endothermic by 1.25 eV, compared to the standard enthalpy change of 0.67 eV. The significant result in studying this coupling is the finding of a high activation barrier for it and the electronic explanation for the barrier. The approximate energies discussed in this work are to be thought of as relative, not absolutely accurate, and as a basis for describing the mechanism–energy diagrams which are qualitatively reasonable.

RESULTS

$CH_2(a)$ Formation from $CH_3(a)$

The methyl group bound to an edge Mo is formally an anion. As shown in the previous study (*12*), it forms easily from methane over twofold coordinatively unsaturated Mo^{IV} by oxidative addition. If H stays on the same Mo as CH_3, it will be a hydride anion and Mo will be formally in the +6 oxidation state. If the hydride moves to a neighboring coordinatively unsaturated Mo^{IV}, then both Mo will be in the +5 oxidation state. If the H shifts to a neighboring S, adsorption will be heterolytic and the methyl anion will be bound to Mo in the +4 oxidation state. In studying methyl dehydrogenation, the adsorbed H from the CH_4 dehydrogenation step is omitted since it does not influence the methyl group oxidation state.

Since a goal of this work is examining the coupling of C_1 species, which will require the presence of adjacent active Mo edge sites, the methyl dehydrogenation is examined in the presence of an adjacent twofold uncoordinated Mo^{IV}. Other recent theoretical work (*16*) on $RuClCH_3$ indicates that such reactions are possible on a single low-coordinate metal center. On MoS_2 an activation energy of 0.7 eV is obtained, which is three times the methane activation energy, but still low. A significant contribution to the activation is the calculated 2.4 eV stronger binding energy of CH_2, which has π component, compared to CH_3 which is only σ bonded (*12*). The structure of the transition state is shown in Fig. 1, and the orbital interactions in the transition state are shown in Fig. 2, where the development of C–Mo π bonding and CH σ donation to Mo are evident. The C–H bond is stretched 0.50 Å compared to 0.29 Å for Mo^{IV} insertion into the methane C–H bond. Assuming the H transfers to a neighboring fully coordinated S^{2-}, the reaction is endothermic by 0.1 eV. The activation energy and endothermicity are close to those found for the Ru complex in Ref. (*16*).

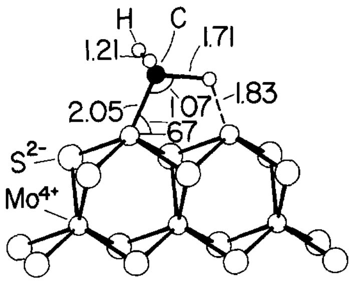

FIG. 1. Transition state for methyl dehydrogenation.

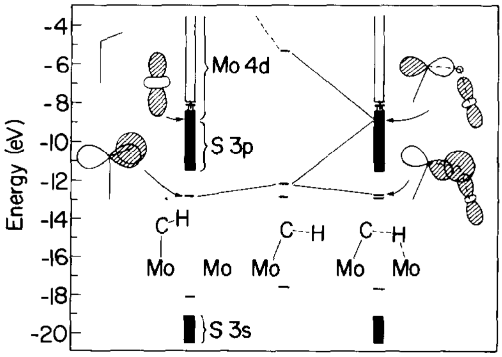

FIG. 2. Orbital interactions in methyl dehydrogenation transition state (Fig. 1) correlated to orbitals of adsorbed methyl. The central column shows CH_3 energy levels for the transition state structure with the right-hand Mo removed.

Mobilities of C_1 Fragments

The formation of CH(a) from CH_2(a) was previously found to be endothermic by 0.6 eV, so its formation is unlikely (*12*). Nevertheless, its activation energy for passing from one twofold coordinatively unsaturated Mo^{IV} to another has been calculated along with those of CH_3 and CH_2. Structures and activation energies given in Fig. 3 suggest that CH_2 will be the most mobile. It rotates 90° to the edge when in the bridge site, thereby maintaining maximum π-type C $2p$ + metal $4d$ overlap with each of the metal centers. The barrier to CH_3 migration is higher because the available p orbital on C has relatively little σ overlap with the two Mo centers in the transition state. CH has the highest barrier since it loses σ bonding and π bonding perpendicular to the edge when in the transition state.

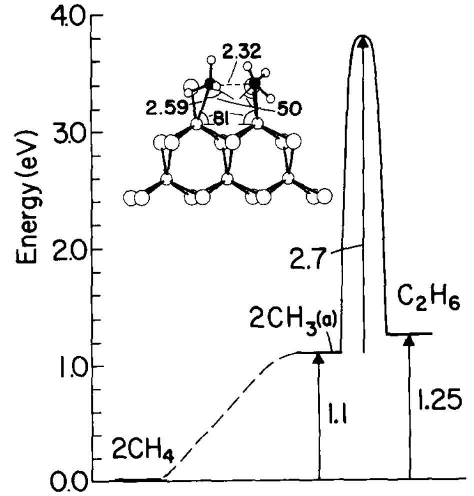

FIG. 4. Ethane formation from CH_3 coupling over two-edge Mo coordinated to 5 *S*. The C are in the plane defined by the Mo–S bonds which are replaced by Mo–C bonds. The pair of angles labeled 50° and 81° have been assigned these values based on the assumption that the two angles in each pair have the same value.

CH_n + CH_m Coupling Mechanisms

It has long been believed that alkyl chain growth in Fischer–Tropsch catalysis on metal surfaces proceeds by the insertion of adsorbed methylene into metal–alkyl bonds. The work of Brady and Pettit (*18*), who decomposed diazomethane over metal surfaces in the presence of H_2, supports this mechanism. Although chain growth over MoS_2 evidently proceeds by CO insertion into Mo–alkyl bonds (*13*), it is still of interest to examine other C_1 coupling schemes to characterize them, for they are also representative of coupling reactions on metal surfaces.

Pathways, transition state structures, and energetics for various ways of coupling CH_2 and CH_3 are shown in Figs. 4–7. Once dissociative adsorption of methane has occurred, all of the pathways are an uphill

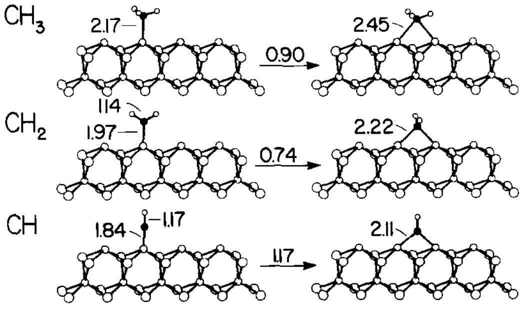

FIG. 3. CH_3, CH_2, and CH binding energy changes and structures in onefold and bridging sites; their bond lengths and angles for the bridging sites are assumed to be the same as the optimized values shown for the onefold sites.

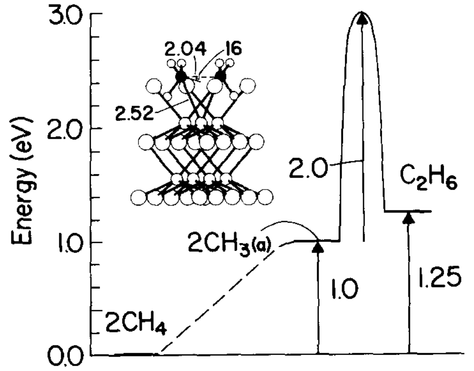

FIG. 5. Ethane formation from CH_3 coupling over an edge Mo coordinated to 4 *S*.

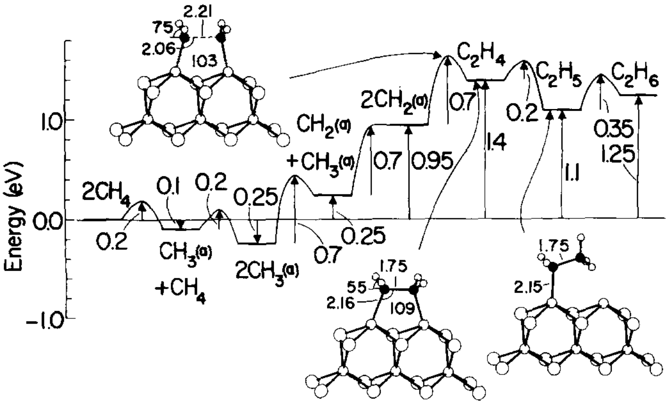

FIG. 6. Ethylene and ethane formation from CH_2 coupling over two Mo coordinated to 4 S.

march to gas-phase ethane and two adsorbed H atoms, with the reaction energy calculated to be endothermic by 1.25 eV. Provided H_2 adsorption is close to reversible, this is consistent with the standard enthalpy change of 0.67 eV for forming C_2H_6 + H_2 from 2 CH_4. Energies for pretransition state steps are determined using the H adsorption energy and the CH_4 activation energy from the earlier study (*12*) and the calculated binding energies of 2.4 and 1.8 eV for the first and second CH_3 binding to adjacent Mo coordinated to 5 S.

Coupling of 2 CH_3 bound to 2 Mo coordinated to 5 S has a high barrier of 2.7 eV (Fig. 4). When the CH_3 are both bound to a single Mo coordinated to 4 S (Fig. 5), the barrier is 0.7 eV less, probably because less Mo–C bond stretching is required in this case. Since 2 CH_3 bound to 2 Mo coordinated to 4 S are about 1 eV more stable than either of the above systems, the barrier would be even higher in this case. The promotion of two electrons in the C–C σ^* orbital to the Fermi level during coupling is shown in Fig. 8. As anticipated by Hoffmann and co-workers (*11*), this promotion causes the high barrier.

The 2 CH_2 couple easily with an activation energy of 0.7 eV to yield adsorbed ethylene on 2 Mo coordinated to 4 S (Fig. 6). This barrier is nearly the reaction energy and is low because ethylene chemisorbs in this di-σ site. Since desorption of the C_2H_4 product costs 1.8 eV, it is understandable why ethylene is not an important product

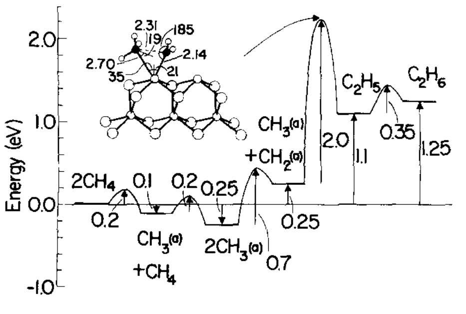

FIG. 7. Ethane formation from CH_3 + CH_2 coupling over two Mo coordinated to 4 S.

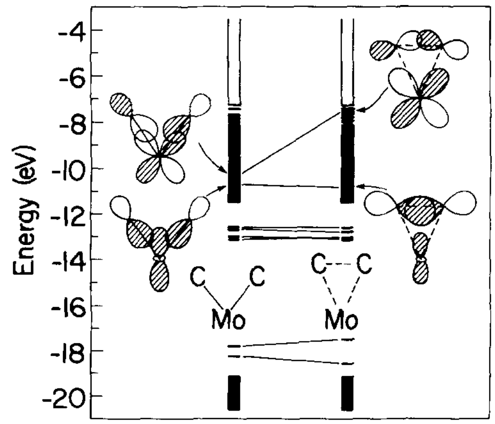

FIG. 8. Orbital correlations for $2CH_3$ bound to Mo coordinated to 5 S and in the transition state shown in Fig. 5.

during Fischer–Tropsch catalysis over MoS_2. Furthermore, it is seen in Fig. 6 that, with the high hydrogen activity of Fischer–Tropsch catalysis, any ethylene that forms should be quickly converted to ethane.

The coupling of CH_2 and CH_3 over 2 Mo that are each coordinated to 4 *S* follows the methylene insertion mechanism, as shown in Fig. 7. The activation energy is 2.0 eV, which is intermediate between the methyl and methylene coupling barriers for this pathway because the ethyl group forms only one σ bond to the edge. The H_3C–Mo distance in the transition state is long, and the overall structure is close to that of the ethyl group product.

The hydrogenation of adsorbed C_2H_5 has not been explicitly calculated. Judging from the CH_4 deydrogenation process, the barrier for this step should be a little greater than the reaction energy to form C_2H_5 from C_2H_6, which is 0.35 eV.

Although Figs. 4–7 show that the formation of ethane and adsorbed H from two methane molecules is endothermic, and all CH_3 and CH_2 coupling reactions to yield ethane are endothermic, it is not to be concluded that the fragments cannot couple on this catalyst under some conditions. When surface H activity is high, Mo–CH_n bond strengths will decrease because of higher Mo coordination than that used in several of the above calculations. Decreases of several tenths of an electron volt in these bond strengths, whether due to high coverage or to calculational errors of this magnitude, would allow coupling. The activation energy for CH_3 coupling will be large enough to prevent this route, but CH_2 coupling to form adsorbed ethylene is calculated to be uphill by only 0.45 eV, so coverage effects and small corrections to the calculated energies could well allow this reaction to occur. If it does, hydrogenation to ethane will clearly be easy. MoS_2 is known to be a hydrogenation catalyst for olefins. Overall, the present calculations support the mechanism proposed by Fischer and Tropsch, wherein CH_2 coupling is the growth mechanism, provided CH_3 and CH_2 can be formed by some means on MoS_2. What is seen here is expected to apply to metal surfaces, where CH_3 coupling will also be retarded by a high activation energy, but CH_2 coupling will be facile, as will be methylene group hydrogenations.

What would make the formation of heavier hydrocarbon molecules from methane possible in principle would be the oxidation of the released hydrogen. The reaction

$$2CH_4 + \tfrac{1}{2}O_2 \rightarrow C_2H_6 + H_2O$$

is highly exothermic with a standard enthalpy charge of −1.83 eV. Controlling this process is the difficulty. Modest yields of C_2 hydrocarbons have been observed over certain oxides, but C_1 oxygenates, including methanol, are the main products (*2*). Methane activation in these cases can be initiated by O^- which are formed chemically, by doping with lower valence cations, or by O 2*p* to metal valence band charge transfer photoexcitation. It is not known whether MoS_2 will polymerize methane in the presence of oxygen.

Adsorption of CO on MoS_2

It has been established by Klier and coworkers (*13*) that Fischer–Tropsch catalysis occurs by CO insertion into Mo–alkyl bonds over MoS_2. Since it is generally believed (*19*) that CO dissociates on metal surfaces in Fischer–Tropsch methanation catalysis, it is of interest to examine CO adsorption and dissociation on MoS_2. From past ASED-MO studies of CO adsorption, it is known that structures and binding sites on metal surfaces are in good agreement with experiment, though adsorption energies are systematically overestimated (*20*). The same is likely to be true for MoS_2.

When bound to an edge in place of S on a Mo coordinated to 5 S, the binding energy of CO is weak (1.5 eV) and the Mo–C distance is long (1.92 Å). This is probably the state of CO seen to desorb at 100°C (*8*). The

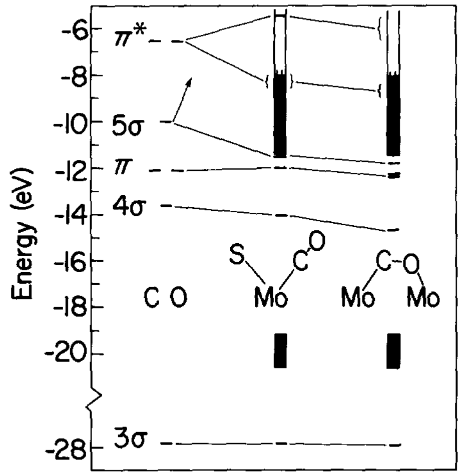

FIG. 9. Orbital correlation diagrams for CO adsorption.

bond is mostly σ, resulting from 5σ donation to the dangling Mo d orbital as shown in Fig. 9; the electrons in the Mo–C σ^* antibonding counterpart orbital are promoted to the conduction band.

The site for dissociative CO adsorption is assumed to have adjacent twofold coordinatively unsaturated Mo atoms. CO binding perpendicular to the edge on one of those sites is strong (3.6 eV) and the Mo–C bond is short (1.84 Å) due to multiple bonding of the Dewar–Chatt–Duncanson type. The di-σ bridging structure is almost as stable (3.45 eV) and a barrier of 0.5 eV is calculated for going from the onefold to the bridging structure. Once in the bridging structure a 0.3 eV activation energy is found for CO dissociation. The stability of the di-σ orientation and the small dissociation barrier are, as for the early d electron-deficient transition metal surfaces (*21*), the result of strong π, 4σ, and 5σ donation to the metal shown in Fig. 9. Experimental studies show that CO is tilted when adsorbed on the Mo(100) surface (*22*). With the high hydrogen activity of Fischer–Tropsch catalysis, the product O will quickly become H_2O which will desorb and C will become CH_3(a). Most of this CH_3 is hydrogenated to methane, but alkanes up to C_5 are detected (*8*). The presence of potassium strongly favors C_1–C_5 alcohol products and reduces the amount of H_2O formed (*8*). It has been found, alternatively, that methane can be formed from methanol decomposition over alkali-promoted MoS_2 (*13*).

It cannot be discounted that, when H_2 is heterolytically adsorbed on MoS_2, CO may insert into Mo–H bonds to form adsorbed formyl, particularly if adjacent fourfold coordinated Mo adsorption sites are scarce. Further hydrogenations and loss of H_2O might then yield adsorbed methyl and methylene groups. Chain propagation might then occur by subsequent CO or CH_2 insertions into metal alkyl bonds. Klier and co-workers (*13*) found different apparent activation energies, 0.70 eV for methanol, 0.98 eV for ethanol, and 1.02 eV for propanol formation over alkali-promoted MoS_2. The lower value for methanol seems inconsistent with the scarcity of examples of hydride to CO transfer reactions (*23*), but under conditions of catalysis over MoS_2 H activity is high, so formyl might be expected to form and its activation energy is expected to be different from that of CO insertion into Mo–CH_2R bonds.

CO Insertion into Mo–CH_3 Bonds and Subsequent Hydrogenations

Klier and co-workers found that when ^{13}C-labeled methanol was injected into the H_2 + CO synthesis gas over alkali-promoted MoS_2, the ^{13}C label always appeared in a terminal position of C_2–C_5 alcohols. From this they proposed that the labeled methanol decomposed to methyl bonded to Mo into which CO inserted. Following hydrogenation, either ethanol desorbed or water was released and subsequent CO insertion into the Mo–ethyl bond resulted in propanol formation, and so on. To model this, CO and CH_3 were bound to a single twofold uncoordinated edge Mo and the transition state shown in Fig. 10 was calculated. The activation energy is low, 0.6 eV, and the insertion products are unstable by

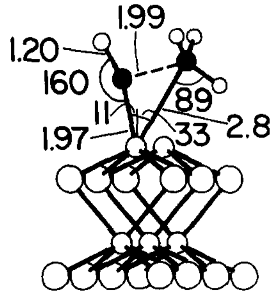

FIG. 10. Transition state structure for CO insertion into a Mo–CH$_3$ bond.

0.45 eV. Hydrogenation to form adsorbed CH_3CHO stabilizes the system by 1.0 eV. Because of the high hydrogen activity during Fischer–Tropsch catalysis, this should occur quickly. A second hydrogenation to form adsorbed CH_3CHOH is destabilizing by 0.6 eV, indicating a weak OH bond, caused by breaking a S–H bond with a strength of 2.65 eV and the reduction of the C–O bond order from 2 to 1. The hydrogenation and desorption of this species as ethanol brings a stability of 0.2 eV. These steps are shown in Fig. 11.

Also shown in Fig. 11 are steps leading from adsorbed CH_3CHOH to desorbed ethane. A second hydrogenation of O and removal of H_2O costs 0.6 eV. Hydrogenation to give adsorbed CH_3CH_2 then brings a stability of 1.15 eV, and a final hydrogenation and removal of ethane costs 0.1 eV.

The formation of ethane and water from methane, carbon monoxide, and hydrogen is exothermic with a standard enthalpy decrease of 1.5 eV. The calculations, based on adsorbed H with a binding energy of 2.65 eV, yield 2.8 eV for this, overestimating experiment because of inaccuracies in the theoretical calculations. Ethanol formation is exothermic with a standard enthalpy of formation of 0.57 eV less and in these calculations it is 0.2 eV less, again because of the approximate theory. The relative results are in agreement with experiment.

Conjecture on the Effect of Potassium in Increasing Alcohol Yield

Potassium added as carbonate markedly increases the ratio of alcohol to alkane Fischer–Tropsch products over MoS$_2$ (*8*, *13*). It has been conjectured that it does this by decreasing the H activity at the catalyst surface (thermodynamic argument, *13*) and, alternatively, by increasing the relative activity of weakly held H (based on thermal desorption studies, *8*). These notions are highly circumstantial and contradictory. A more specific alternative is proposed here.

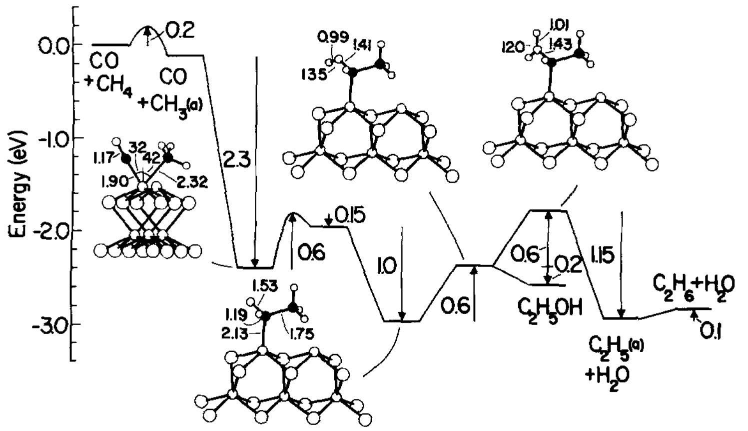

FIG. 11. Pathways, structures, and energetics for ethanol and ethane formation by the mechanisms of CO insertion into the Mo–CH$_3$ bond followed by subsequent hydrogenation using H bound to the catalyst with an assumed energy of 2.65 eV. The Mo–C and C–C distances for CH_3CHOH(ads) and CH_3CHOH_2(ads) are assumed to be the same as for CH_3CHO(ads).

Potassium will be present in cationic form associated with carbonate anions on the catalyst surface. It would seem likely that K^+ would be able to interact with O in $CH_3CHO(a)$ and $CH_3CHOH(a)$, and block or at least slow the rate of hydrogenation and H_2O formation. Using estimated K^+ 4*s* parameters, 6.34 eV for the ionization potential, and 1.17 a.u. for the Slater exponent, K^+ is found to bind with an energy of 0.45 eV to O in $CH_3CHO(a)$. The binding in fact should be stronger because ASED-MO calculations underestimate ionic interactions. The K–O distance is 1.85 Å and the K–O–C angle 125°. It is conjectured, therefore, that K^+ may be stabilizing surface alkoxy intermediates, selectively favoring alcohol formation to alkane formation during Fischer–Tropsch catalysis over MoS_2.

Concluding Comments

In this study molecular orbital theory has been used as a guide to structures and mechanisms for the formation of CH_n from CH_4 over MoS_2, $CH_n + CH_m$ couplings, CO adsorption and dissociation, and CO insertion into Mo–CH_3 followed by hydrogenations to C_2H_6 and CH_3CH_2OH. The $CH_n + CH_m$ couplings have, as expected, high activation energies because of electron promotion to the Fermi level during C–C bond formation. Furthermore, C–C bonds, once formed, are not strong enough to make C_2H_4 or C_2H_6 formation possible, which is in agreement with the thermodynamics for CH_4 coupling in the absence of stabilizing ancillary reactions such as H_2O formation. In the presence of appropriate H consuming reactions, it can be concluded that the most probable coupling reaction will be CH_2 to yield strongly adsorbed C_2H_4 which can readily be hydrogenated to C_2H_6.

Weakly held CO is predicted for fivefold coordinated Mo and this seems to correspond to the experimentally observed thermal desorption peak at 100°C. In the Fischer–Tropsch process HCO formation at such sites and subsequent hydrogenations and CO insertion products to yield the observed C_1–C_5 products can be considered. However, only a few Mo sites of fourfold coordination could allow other mechanisms and such sites may be fluctuating in nature, due to H_2 and H_2S reactions and S mobility at crystal edges. A single 4-coordinated Mo has the ability to hold CH_3 and allow CO to insert into the Mo–CH_3 bond with a low activation barrier. Subsequent hydrogenation mechanisms were beyond the scope of this study, but the calculated structures and stabilities of hydrogenated intermediates are sensible and alcohol and alkane product stabilities are in qualitative agreement with experiment. The ability of K^+ to stabilize oxygenated intermediates and block hydrogenation to H_2O is proposed, based on a rough calculation of the binding of K^+ to O in $CH_3CHO(a)$.

Whether or not CH_4 can be incorporated in Fischer–Tropsch reactions over MoS_2 can only be answered by experimental work. Such an investigation is encouraged for MoS_2 and also WS_2 which has similar catalytic properties.

ACKNOWLEDGMENT

This work has been supported by the Gas Research Institute.

REFERENCES

1. McGhee, W. D., and Bergman, R. G., *J. Amer. Chem. Soc.* **110,** 4246 (1988).
2. Shvets, V. A., Vorotyntsev, V. M., and Kazansky, V. B., *Kinet. Katal.* **10,** 356 (1969); Kazansky, V. B., *Kinet. Katal.* **18,** 43 (1977); Lipatkina, N. I., Shvets, V. A., and Kazansky, V. B., *Kinet. Katal.* **19,** 979 (1978); Kaliaguine, S. L., Shelimov, B. N., and Kazansky, V. B., *J. Catal.* **55,** 384 (1978); Liu, R.-S., Iwamoto, M., and Lunsford, J. H., *J. Chem. Soc. Chem. Commun.* 78, (1982); Liu, H.-F., Liu, R.-S., Liew, K. Y., Johnson, R. E., and Lunsford, J. H., *J. Amer. Chem. Soc.* **106,** 4117 (1984); Ito, T., Wang, J.-X., Lin, C.-H., and Lunsford, J. H., *J. Amer. Chem. Soc.* **107,** 5062 (1985); Ito, T., and Lunsford, J. H., *Nature (London)* **314,** 721 (1985); Driscoll, D. J., Martir, W., Wang, J.-X., and Lunsford, J. H., *J. Amer. Chem. Soc.* **107,** 58 (1985); Driscoll, D. J., and Lunsford, J. H., *J. Phys. Chem.* **89,** 4415 (1985).
3. Anderson, A. B., and Ray, N. K., *J. Amer. Chem. Soc.* **107,** 253 (1985); Mehandru, S. P., Anderson,

A. B., and Brazdil, J. F., *J. Chem. Soc. Faraday Trans. I* **83,** 463 (1987); Mehandru, S. P., Anderson, A. B., Brazdil, J. F., and Grasselli, R. K., *J. Phys. Chem.* **91,** 2930 (1987); Wand, M. D., Brazdil, J. F., Mehandru, S. P., and Anderson, A. B., *J. Phys. Chem.* **91,** 6515 (1987); Mehandru, S. P., Anderson, A. B., and Brazdil, J. F., *J. Amer. Chem. Soc.* **110,** 1715 (1988).

4. (*a*) Tibbetts, G. G., *J. Cryst. Growth* **66,** 632 (1984); *J. Cryst. Growth* **73,** 431 (1985); (*b*) Wright, P. G., Ashmore, P. G., and Kemball, C., *Trans. Faraday Soc.* **54,** 1692 (1958); Schouten, F. C., Kaleveld, E. W., and Bootsma, G. A., *Surf. Sci.* **63,** 460 (1977); Lee, M. B., Yang, Q. Y., Tang, S. L., and Ceyer, S. T., *J. Chem. Phys.* **85,** 1693 (1986); Beebe, T. P., Jr., Goodman, D. W., Kay, B. D., and Yates, J. T., Jr., *J. Chem. Phys.* **87,** 20 (1987); Schouten, F. C., Gijzeman, O. L. J., and Bootsma, G. A., *Surf. Sci.* **87,** 1 (1979); Hamza, A. V., and Madix, R. J., *Surf. Sci.* **179,** 25 (1987); Gaidai, N. A., Babernich, L., and Guczi, L., *Kinet. Katal.* **15,** 974 (1974); Kuijpers, E. G. M., Jansen, J. W., van Dillen, A. J., and Geus, J. W., *J. Catal.* **72,** 75 (1981); Firment, L. E., and Somorjai, G. A., *J. Chem. Phys.* **66,** 2901 (1977); Szuromi, P. D., Engstron, J. R., and Weinberg, W. H., *J. Phys. Chem.* **89,** 2497 (1985).
5. Anderson, A. B., and Maloney, J. J., *J. Phys. Chem.* **92,** 809 (1988).
6. Okuhara, T., and Tanaka, K., *J. Phys. Chem.* **82,** 1953 (1978); Tanaka, K., and Okuhara, T., *J. Catal.* **78,** 155 (1982); Hall, W. K., *in* "Proceedings, Fourth International Conference on the Chemistry and Uses of Molybdenum" (H. F. Barry, and T. C. H. Mitchell, Eds.), p. 224. Climax Molybdenum Co., Ann Arbor, MI, 1982.
7. Okuhara, T., Tanaka, K., and Miyahara, K., *J. Catal.* **48,** 229 (1977); Hall, W. K., and Millman, W. S., *in* "Proceedings, 7th International Congress on Catalysis, Tokyo, 1980" (T. Seiyama and K. Tanabe, Eds.), Part B, p. 1304. Elsevier, Amsterdam, 1981.
8. Dianis, W. P., *Appl. Catal.* **30,** 99 (1987).
9. Anderson, A. B., Al Saigh, Z. Y., and Hall, W. K., *J. Phys. Chem.* **92,** 803 (1988).
10. Blackburn, A., and Sermon, P. A., *J. Chem. Technol. Biotechnol. Chem. Technol. A* **33,** 120 (1983); Sampson, C., Thomas, J. M., Vasudevan, S., and Wright, C., *J. Bull. Soc. Chim. Belg.* **90,** 1215 (1981); Wright, C. J., Fraser, D., Moyes, R. B., and Wells, P. B., *Appl. Catal.* **1,** 491 (1981); Wright, C. J., Sampson, C., Fraser, D., Moyes, R. B., and Wells, P. B., *J. Chem. Soc. Faraday Trans. I* **76,** 1585 (1980).
11. Zheng, C., Apeloig, Y., and Hoffmann, R., *J. Amer. Chem. Soc.* **110,** 749 (1988).
12. Anderson, A. B., Maloney, J. J., and Yu, J., *J. Catal.* **112,** 392 (1988).
13. Klier, K., Herman, R. G., Nunan, J. G., Smith, K. J., Bogdan, C. E., Young, C.-W., and Santiesteban, J. G., *in* "Methane Conversion" (D. M. Bibby, C. D. Chang, R. F. Howe, and S. Yurchak, Eds.), Elsevier, Amsterdam, 1988; Santiesteban, J. G., Bogdan, C. E., Herman, R. G., Nunan, J. G., and Klier, K., *in* "Proceedings, 9th International Congress on Catalysis, Calgary, 1988" (M. J. Phillips and M. Ternan, Eds.), Chem. Institute of Canada, Ottawa.
14. Anderson, A. B., *J. Chem. Phys.* **62,** 1187 (1975).
15. Anderson, A. B., Grimes, R. W., and Hong, S. Y., *J. Phys. Chem.* **91,** 4245 (1987).
16. Carter, E. A., and Goddard, W. A., III, *J. Amer. Chem. Soc.* **109,** 579 (1987).
17. Fischer, F., and Tropsch, H., *Brenst. Chem.* **7,** 97 (1926); *Chem. Ber.* **59,** 830 (1926).
18. Brady, R. C., III, and Pettit, R., *J. Amer. Chem. Soc.* **103,** 1287 (1981).
19. Vannice, M. A., and Garten, R. L., *J. Catal.* **56,** 236 (1979); Vannice, M. A., and Garten, R. L., *J. Catal.* **66,** 242 (1980); Bartholomew, C. H., Pannell, R. B., and Butler, J. L., *J. Catal.* **65,** 335 (1980); Kao, C.-C., Tsai, S.-C., and Chung, Y.-W., *J. Catal.* **73,** 136 (1982); Burch, R., and Flambard, A. R., *J. Catal.* **78,** 389 (1982); Vannice, M. A., *J. Catal.* **74,** 199 (1982).
20. Anderson, A. B., and Awad, Md. K., *J. Amer. Chem. Soc.* **107,** 7854 (1985).
21. Mehandru, S. P., and Anderson, A. B., *Surf. Sci.* **169,** L281 (1986); Anderson, A. B., and Dowd, D. Q., *J. Phys. Chem.* **91,** 869 (1987); Mehandru, S. P., and Anderson, A. B., *Surf. Sci.* **201,** 345 (1988).
22. Fulmer, J. P., Zaera, F., and Tysoe, W. T., *J. Chem. Phys.* **87,** 7265 (1987); Moon, D. W., Cameron, S., Zaera, F., Eberhardt, W., Carr, R., Bernasek, S. L., Gland, J. L., and Dwyer, D. J., *Surf. Sci.* **180,** L123 (1987).